Anisotropic rheology and directional mechanotransduction in vascular endothelial cells

Juan C. del Álamo*, Gerard N. Norwich[†], Yi-shuan Julie Li[†], Juan C. Lasheras*[†‡], and Shu Chien[†‡§]

Departments of *Mechanical and Aerospace Engineering, [†]Bioengineering, and [§]Medicine, University of California at San Diego, La Jolla, CA 92093

Contributed by Shu Chien, July 15, 2008 (sent for review May 15, 2008)

Adherent cells remodel their cytoskeleton, including its directionality, in response to directional mechanical stimuli with consequent redistribution of intracellular forces and modulation of cell function. We analyzed the temporal and spatial changes in magnitude and directionality of the cytoplasmic creep compliance (Γ) in confluent cultures of bovine aortic endothelial cells subjected to continuous laminar flow shear stresses. We extended particle tracking microrheology to determine at each point in the cytoplasm the principal directions along which Γ is maximal and minimal. Under static condition, the cells have polygonal shapes without specific alignment. Although Γ of each cell exhibits directionality with varying principal directions, Γ averaged over the whole cell population is isotropic. After continuous laminar flow shear stresses, all cells gradually elongate and the directions of maximal and minimal Γ become, respectively, parallel and perpendicular to flow direction. This mechanical alignment is accompanied by a transition of the cytoplasm to be more fluid-like along the flow direction and more solid-like along the perpendicular direction; at the same time Γ increases at the downstream part of the cells. The resulting directional anisotropy and spatial inhomogeneity of cytoplasmic rheology may play an important role in mechanotransduction in adherent cells by providing a means to sense the direction of mechanical stimuli.

anisotropy | microrheology | shear stress

Blood vessels are exposed to flow-induced shear stresses, which are borne primarily by vascular endothelial cells (VECs) (1). VECs perform functions such as regulation of permeability, the production, secretion, and metabolism of biochemical substances, and modulation of vascular smooth muscle cell contractility. Sustained application (hours) of laminar shear stresses (LSS) to cultured VECs induces cell elongation and alignment along the flow direction (2). The actin stress fibers thicken and gradually align with flow (3), the focal adhesions relocate primarily to the upstream part of the cell (4), and cell–cell junctions are transiently disrupted (5). The structural reorganization of cytoskeleton leads to changes in subcellular microrheology that can play an important role in mechanosensing and signaling by redistributing the external forces among intracellular subdomains (6, 7). Existing evidence suggests that changes in subcellular microrheology, including directionality and polarity, could provide a mechanism for cells to sense external forces and their direction, modulate intracellular signaling, and regulate gene expression and cell turnover (8).

The realization that mechanical polarity may modulate cell function has conferred special significance to measuring the spatiotemporal adaptation of rheological properties of VECs to shear stresses. Sato *et al.* (9) determined the viscous and elastic resistances to micropipette aspiration of VECs after 24 h of directional LSS and provided the first quantitative evidence of the adaptation of VEC mechanical properties to shear stresses, but the aspiration involved relatively large cell deformation (10). Characterization of subcellular changes is needed to understand how cytoskeletal reorientation translates into spatial and directional changes in microrheological properties of VECs. Atomic force microscopy (AFM) has revealed that VECs become more resistant to indentation by AFM tip 6–24 h after the application of a LSS of 20 dyn/cm^2, with a transient asymmetry between upstream and downstream parts (11). More recently, particle tracking microrheology (PTM) has been used to investigate the temporal changes in viscoelastic shear moduli of cells in the plane of application of LSS over time courses of seconds (12) and minutes (13). These studies, however, do not address the adaptation of the in-plane microrheological properties of VECs to LSS applied over periods of hours (i.e., the time scale of morphological remodeling), nor the anisotropy of this adaptation, which correlates strongly with the direction of the applied LSS, as shown in this article.

Our work was motivated by the need to measure in a noninvasive way the temporal changes in magnitude, direction, and spatial distribution of rheological properties of VECs subject to prolonged exposure to LSS. We used directional particle tracking microrheology (DPTM), an extension of PTM (14, 15) that analyzes the Brownian dynamics of intracellular particles by measuring the 2×2 correlation tensor of particle displacements (16). DPTM allowed us to determine at each instant of time the directions along which the cytoplasmic creep compliance (Γ) is maximal and minimal (principal directions) at each location.

Results

The Mitochondria as Endogenous Probes for DPTM. Being compact and connected to the cytoskeleton (17), the mitochondria have long been used as endogenous probes to measure intracellular mechanical properties (18, 19). We tracked and analyzed the random motion of these organelles to determine the magnitude and anisotropy of the microrheological properties of VECs subjected to continuous LSS (see *Materials and Methods* and Fig. 1). We accounted for the dynamics and geometry of the mitochondria and corrected for possible sources of artifactual directionality. One of these sources is the persistent motion of some mitochondria due to transport by motor proteins on cytoskeletal tracks. This directed transport has been associated to ATP-dependent superdiffusive dynamics and an increased mobility (20, 21). Directed transport, in contrast to Brownian motion, is anisotropic at long τ. This effect can be seen in the mean square displacements (MSD) of a particle in an orthotropic medium being transported at a constant velocity (V), and subject to a Brownian motion with diffusion coefficients D_+ and D_- along the principal directions of the medium. It follows in this simple directed-Brownian model that the principal values of the MSD (PMSD) are $r_+^2 = (V\tau)^2 + D_+\tau$, and $r_-^2 = D_-\tau$. Thus, the anisotropy of the MSD (A_{MSD}) increases as

Author contributions: J.C.d.Á., J.Y.-S.L., J.C.L., and S.C. designed research; J.C.d.Á., G.N.N., and J.Y.-S.L. performed research; J.C.d.Á., G.N.N., and S.C. analyzed data; and J.C.d.Á., J.C.L., and S.C. wrote the paper.

The authors declare no conflict of interest.

[‡]To whom correspondence should be addressed. E-mail: shuchien@ucsd.edu.

This article contains supporting information online at www.pnas.org/cgi/content/full/0804573105/DCSupplemental.

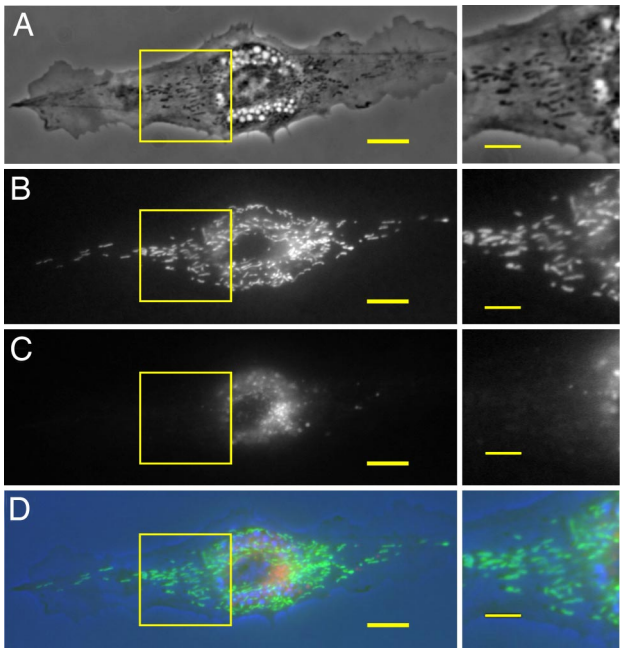

Fig. 1. Staining for different organelles and vesicles in the same VEC reveals that the endogenous particles used in our experiments are the mitochondria. (*A*) Phase image; (*B*) mitochondria marked with MitoTracker Green FM (Invitrogen); (*C*) lysosomes marked with Lysotracker Red DND-99 (Invitrogen); (*D*) merged image composed by using panels (*A*, *B* and *C*) in the blue, green and red channels, respectively. The images at the right of each panel show magnifications of the framed area in the corresponding left panel. The scale bars are 5 μm in left panels and 2 μm in right panels.

$$\frac{r_+^2}{r_-^2} = \frac{D_+}{D_-}\left(\frac{\tau}{T}+1\right), \qquad [1]$$

where $T = D_+/V^2$ is the timescale over which transport dominates diffusion. As predicted by the model, A_{MSD} of the mitochondria undergoing superdiffusive directed transport ($V > 0$) shows a linear increase with τ (Fig. 2). After removal of the particles undergoing direct transport from the analysis, the PMSD for the remaining particles ($V = 0$) show a level of anisotropy between 3 and 5 that varies little with τ, as expected from a passive orthotropic medium. The model also predicts that the degrees of A_{MSD} of the mitochondria showing these two types of behaviors should converge as τ approaches 0, and this is indeed the case (Fig. 2, *Inset*).

A second possible source of artifactual directionality that was ruled out in our analysis is the fact that mitochondria have ellipsoidal shapes rather than being perfect spheres, as this may affect their random thermal motion. At short τ, the Brownian motion of an ellipsoid is directional even in isotropic media because its drag coefficient is smaller when moving along its major axis (22). At longer τ, however, the random rotation of the ellipsoid renders its motion isotropic and statistically indistinguishable from that of a sphere. The transition from anisotropic to isotropic behavior occurs at $\tau \sim 1/D_\vartheta$, where D_ϑ is the rotational diffusion coefficient of the ellipsoid. Such transition would appear as a decrease in A_{MSD} with increasing τ, which is not observed in our measurements (Fig. 2). Therefore, our results indeed reflect the anisotropy of the microrheological properties of VECs and are not affected by the ellipsoidal shape of the mitochondria. This important point was further confirmed

¶This linear growth holds in the range 0.2 s $< \tau <$ 10 s in which Γ has been measured, but it should saturate for $\tau > T_V$, where T_V is the typical duration of the directed walks.

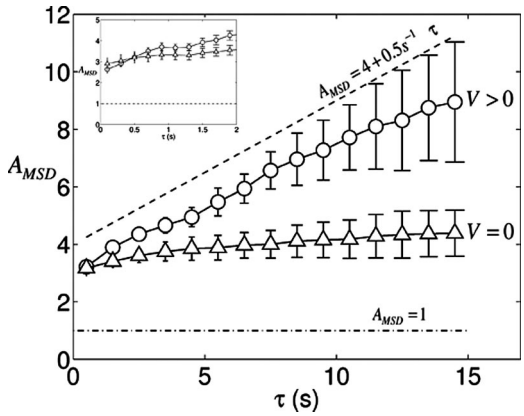

Fig. 2. A_{MSD} (Eq. 1) of the mitochondria of VECs ($n = 8$), represented as a function of time separation τ. Open circles, particles undergoing active motion ($r_+^2 = V^2\tau^2 + D\tau$ with $V > 0$); open triangles, particles undergoing passive motion ($V = 0$). The chain-dotted line indicates isotropy, $A_{\mathrm{MSD}} = 1$, whereas the dashed line represents anisotropy increasing as $A_{\mathrm{MSD}} = 4 + 0.5\ \mathrm{s}^{-1}\ \tau$. (*Inset*) Evolution of A_{MSD} for short τ. Error bars indicate S.D.

by the agreement we found between the DPTM measurements using endogenous probes presented here and additional experiments conducted with exogenous, 0.2 μm-diameter polystyrene microspheres introduced into the VECs.

Anisotropy of the Microrheological Properties of VECs. Fig. 3 shows the averaged PMSD of the mitochondria in a VEC culture before the application of LSS. Consistent with Fig. 2*B*, the average values of r_+^2 are larger than r_-^2 by a factor of 3–5. Because $\Gamma_{+,-}$ are directly proportional to the PMSD (see DPTM in *Materials and Methods*), these results indicate that, at each point in the cytoplasm, there is a direction along which Γ is 3–5 times higher than in the direction perpendicular to it. The degree of anisotropy of Γ increases slightly with an increase in τ. The power slopes of $r_+^2(\tau)$ and $r_-^2(\tau)$, i.e., β_+ and β_-, respectively (Fig. 3, *Inset*), indicate how closely the cytoplasm behaves as a viscous fluid ($\Gamma \propto \mathrm{MSD} \propto \tau^\beta$, with $\beta = 1$) or as an elastic network ($\beta = 0$) along each principal direction. For $\tau <$ 1 s, both slopes are similar and $\beta \approx 0.45$, consistent with an elastic-like regime in all directions. However, the power slopes of $r_+^2(\tau)$ and $r_-^2(\tau)$ diverge for $\tau > 1$ s, where $\beta_+ \approx 0.85$ and $\beta_- \approx 0.50$, showing that each point of the cytoplasm behaves more like a

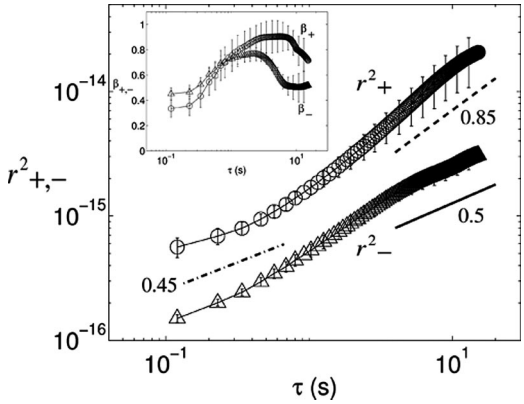

Fig. 3. PMSD of the mitochondria of VECs ($n = 8$), represented as a function of time separation τ. Open triangles, PMSD along the direction of minimal compliance (r_-^2); copen circles, PMSD along the direction of maximal compliance (r_+^2). The chain-dotted, solid and dashed straight lines have power slopes $\beta \approx 0.45$, 0.50 and 0.85, respectively. (*Inset*) Power slopes of the PMSD, β_+ and β_-, as a function of τ. Error bars indicate S.D.

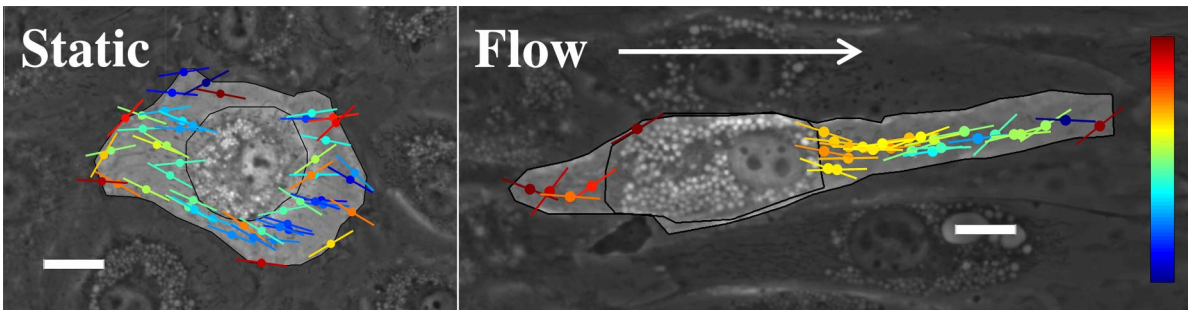

Fig. 4. Magnitude and directionality of creep compliance (Γ) at different positions of two VECs. (*A*) Before application of continuous LSS. (*B*) Twenty-four hours after starting LSS. Circles indicate the average position of each tracked marker; the segments are oriented parallel to the direction of maximum Γ at each point at $\tau = 1$ s. The circles and segments are colored according to the logarithm of MSD of corresponding markers. Hot and cold colors indicate respectively low and high Γ.

viscous fluid along one direction and more like an elastic network along the direction perpendicular to that. The same conclusions are drawn from the analysis of the shear modulus [supporting information (SI)].

The anisotropic microrheology of individual cells brings up the question how the principal directions are distributed spatially throughout the cytoplasm. Fig. 4*A* shows an example of the regional variations in Γ in one cell under static condition. Consistent with this result, the rose histograms of the angle of maximum Γ (α_+) compiled from all of the probes in each one of eight cells (Fig. 5*A*) show 1 or 2 distinct preferential orientations. When averaged over a large population of cells, however, the overall distribution of α_+ is isotropic in the absence of flow, showing no preferential orientation of PMSD (Fig. 5*B*).

Reorientation of the Microrheological Properties of VECs Resulting from Shear Stresses. Fig. 6 displays the 24-h variation of the distribution of the principal directions of Γ for $\tau = 1$ s in a VEC culture kept in static condition (Fig. 6*A*), compared with another subjected to continuous LSS (Fig. 6*B*). The results indicate that when VECs are subjected to sustained LSS, the principal directions of Γ of their cytoplasm align gradually with flow. The distribution of α_+ in the VEC culture is no longer uniform 24 h after sustained LSS. Instead, it becomes narrowly distributed such that $\alpha_+ \approx 0$, which is the direction of the LSS. This realignment takes place at all points of the cytoplasm, as seen in the example cell of Fig. 4*B*, and also at all values of τ in the range investigated, as shown in Fig. 6*C* for $\tau = 10$ s. Tracking the same cell at different times after flow initiation shows that the distribution of α_+ after 6 h of LSS has converged substantially with a peak at $\alpha_+ = 0$, indicating the effective completion of the reorientation process (Fig. 7*A*). The same analysis on VECs under static condition (Figs. 6*B* and 7*B*) shows no reorientation of the microrheological properties, either when averaged over the whole population or for individual cells in the culture.

Evolution of the Magnitude of the Microrheological Properties of VECs Resulting from Shear Stresses. The reorientation of the microrheological properties of VECs in response to the direction of the applied LSS is accompanied by a polarization of the magnitude of Γ in the same direction. Fig. 8 reveals that after 24 h of continuous flow, there is an increase of the MSD of mitochondria and hence an increase in Γ, localized in the downstream side of the cells. This spatial polarization can also be seen in the single cell shown in Fig. 4*B*. As expected, the VECs under static condition show no signs of polarization of their rheological properties (Figs. 4*A* and 8).

The time evolution of the PMSD of mitochondria in VECs subjected to continuous LSS shows a gradual increase in the value of r_+^2 (Fig. 9*A*); this does not occur in the control static case (Fig. 9*B*). Thus, 24 h after the continuous application of LSS, $r_+^2(\tau = 1\text{ s})$ is $\approx 2\times$ that in the static case ($P < 0.01$), which is in agreement with Fig. 8. This evolution of r_+^2 with time is prominent with longer τ and becomes nearly negligible with $\tau < 0.5$ s. Together with Figs. 6*A* and 7*A*, these results suggest that the cytoplasm of VECs becomes more compliant in the direction of the applied flow. On the other hand, the PMSD along the stiff direction (Fig. 9*B*) shows smaller variations which are not statistically significant when compared with the control static case. The behavior of the slope of the PMSD shows interesting differences between the shear flow and the static case. Fig. 9*B* indicates that the viscoelastic character of the cytoplasm of VECs under static condition does not exhibit any sign of remodeling in either the soft or the stiff direction. In contrast, Fig. 9*A* indicates that the cytoplasm of the VECs subjected to sustained LSS becomes gradually more viscous-fluid-like along the soft direction, as the slope of r_+^2 gradually increases with time after the application of shear flow. The analysis of the shear modulus leads to the same results (SI).

Discussion

It is generally accepted that the cytoskeleton of adherent cells plays a fundamental role in mechanotransduction by redistributing across the cytoplasm the external mechanical loads that are applied to the cells in terms of forces and displacements (6–8). The magnitude of the constitutive mechanical properties of the cell (elastic modulus, shear modulus, etc.) is important for this process because it sets the level of intracellular force/

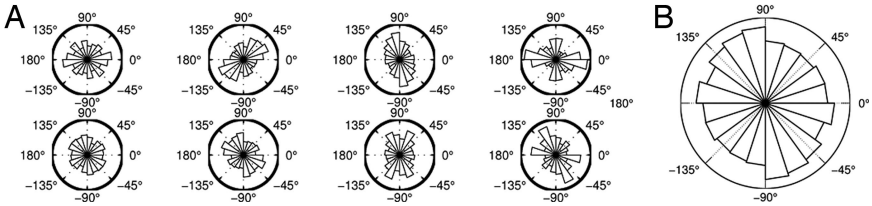

Fig. 5. Distribution of the angles, α_+, of the direction of maximum compliance in VECs under static condition for single cells (*A*) and averaged for a population ($n = 8$) (*B*). The data were obtained from PMSD at $\tau = 1$ s. All distributions are normalized to yield the same area.

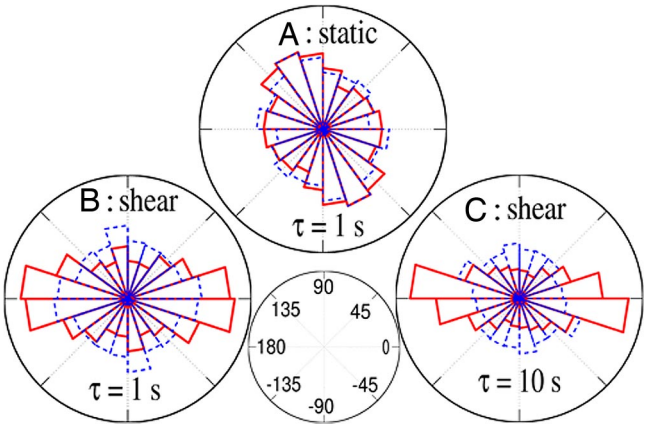

Fig. 6. Distribution of α_+ for VECs at t = 0 h (dashed blue, $n = 4$) and t = 24 h (solid red, $n = 16$), for different time separations, τ. (*A*) static condition, $\tau = 1$ s. (*B–C*) Continuous flow along the direction $\alpha = 0$ at $\tau = 1$ s (*B*) and 10 s (*C*). All distributions are normalized to yield the same area.

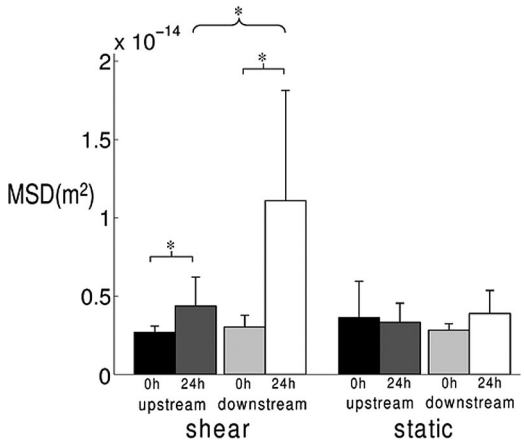

Fig. 8. Variation of average MSD in the upstream and downstream parts of VECs subjected to continuous LSS (*Left*) and under static condition (*Right*). *, $P < 0.01$.

deformation in response to a given external mechanical load. Therefore, its measurement has received considerable attention (9, 11–13, 15, 19, 21, 23). The anisotropy of the constitutive mechanical properties is also important because it provides the cell with a mechanism to translate external mechanical loads differently depending on their direction. However, there are very few studies that have produced quantitative measurements of this anisotropy for adherent cells (19, 24), and there is still no information on how the degree of anisotropy is modified when the cells undergo remodeling in response to external mechanical stimuli. The modification of anisotropy is relevant to physiological situations where cells are subject to sustained external forces that have a given direction, e.g., blood flow on VECs or air flow on airway epithelial cells. We have used DPTM to measure the magnitude and especially the anisotropy of the microrheological properties of the cytoplasm of VECs subjected to a continuous LSS of 16 dyn/cm^2.

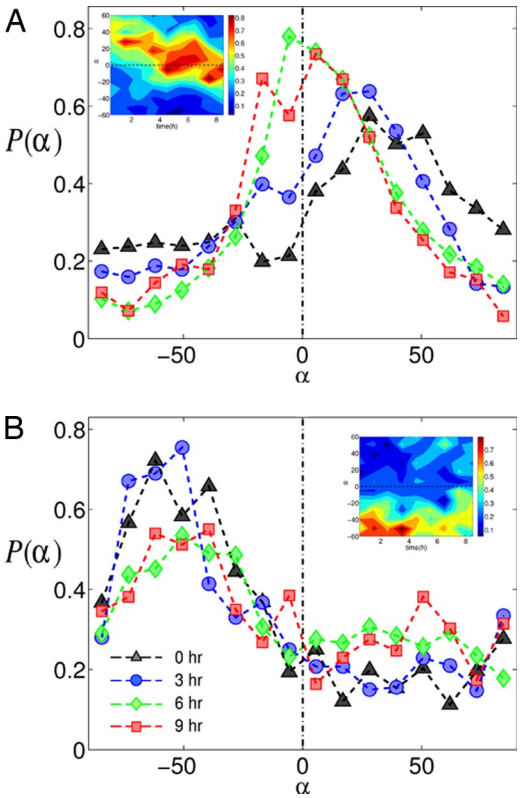

Fig. 7. Time evolution of distribution of α_+ for single cells, $p(\alpha_+|t)$. Each line shows $p(\alpha_+|t)$ for the same cell at a different times, *t*. The black (filled triangles) curve represents the initial state ($t = 0$), while blue (filled circles), green (filled squares) and red (filled diamonds) curves were obtained 3, 6, and 9 h, respectively, after starting the experiment. The data were obtained from PMSD at $t = 1$ s. All distributions are normalized to yield the same area. (*Insets*) Higher-time-resolution, 2D plots of $p(\alpha_+|t)$ where the abscissa is time and ordinate is α_+.

Our results indicate that, before the application of LSS, the cytoplasm of individual VECs is already anisotropic, showing at each location a softer direction along which Γ is 3–5 times larger than in the direction perpendicular to it. Thus, the spatial distribution of the principal directions of Γ occurs at the level of individual cells, even in a static condition, and it is observed for all time separations investigated ($0.2 \text{ s} < \tau < 10$ s). However, there is no preferential orientation among all cells in the total population in a confluent VEC monolayer. For time separations $0.2 \text{ s} < \tau < 1$ s, the response of the cytoplasm is elastic-like in all directions. At longer time separations, a viscous-like regime is observed in the softer direction, while the stiffer direction remains more elastic in nature. The transition between an elastic regime at short τ and a viscous regime at $\tau \approx 1$ s has been previously observed for different types of living cells (12, 15, 25–28). Recently, a similar transition has been attributed to nondirected ATP-dependent processes in isotropic networks cross-linked with motor proteins (29, 30). The possible interplay between microrheological anisotropy of the cell and nondirected ATP-dependent processes remains to be studied theoretically and experimentally.

In the present study, we have shown that the remodeling of VECs subjected to continuously applied LSS is such that, at each position within the cell, the direction more compliant to shear deformation gradually aligns parallel to the flow. This remodeling process requires approximately 6 h for the level of shear stress and the experimental conditions used in this study. These results are consistent with previous observations that 6–24 h after the application of continuous LSS, the actin stress fibers of the VECs become thicker and align in the flow direction (3, 31, 32), but the overall density of polymerized actin decreases (33). While the thicker stress fibers aligned with flow direction could withstand higher extensional loads, the rest of the cytoskeletal network would be sparser and therefore more compliant to the shear deformation as shown by the larger MSD in the thermal random motion of small intracellular markers in this direction.

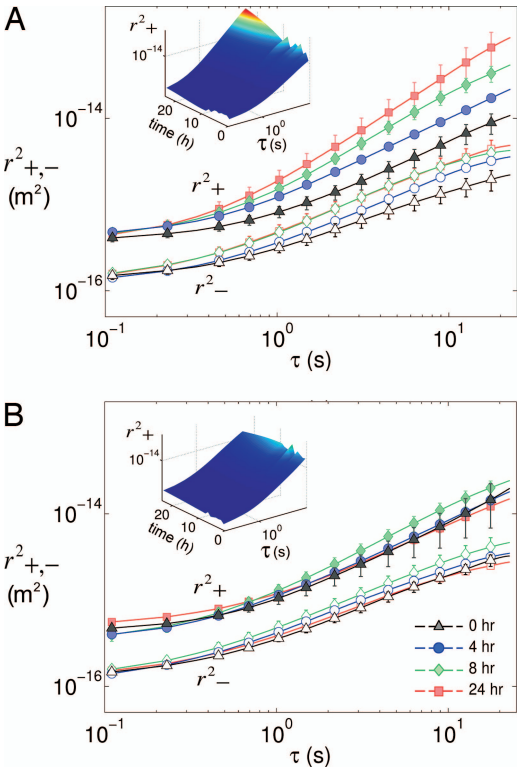

Fig. 9. Time evolution of PMSD of VECs subjected to continuous LSS (*A*) or under static condition (*B*). The curves for r_+^2 are plotted with solid symbols *A* and *B Upper*, and those for r_-^2 are plotted with open symbols in *Lower*. The black triangles represent the initial state (t = 0), whereas blue circles, green squares and red diamonds denote 4, 8, and 24 h, respectively, after starting the experiment. (*Insets*) 3D representations of $r_+^2(\tau, t)$.

Hu *et al.* (19, 24) have reported that the mechanical force imposed by magnetic twisting cytometry (MTC) loads the actin stress fibers over long distances and that the resistance to this multicomponent load is higher in the direction parallel to the fibers. The inhomogeneous, anisotropic picture arising from these experiments suggests that results obtained using different rheological techniques are complementary, and one should exercise caution in interpreting each of them. In the homogeneous isotropic simplification, all of the nonzero components of the $3 \times 3 \times 3 \times 3$ tensor that relates stress and strain are proportional to each other, and therefore the relation between applied stresses and measured strains is the same regardless of the way the stresses are applied. However, this property is no longer true for inhomogeneous, anisotropic media such as the cytoplasm of adherent cells studied here, where each technique measures different components of the complex viscoelasticity tensor. Consistent with these ideas, a recent survey has shown that the rheological properties of adherent cells measured from PTM differ systematically from the properties measured with MTC and AFM (21).

The only available DPTM data for a biological sample are those of Hasnain and Donald (16), who reported that the shear modulus of a sheared DNA solution is lower in the direction parallel to the DNA fibers than in the perpendicular direction for angular frequencies $\omega < 15\ s^{-1}$. This behavior is consistent with our measurements, which take place in an interval of time separations that corresponds to $0.1\ s^{-1} < \omega < 5\ s^{-1}$, and thus is also in the range of $\omega < 15\ s^{-1}$. The cross-over reported for higher frequencies by Hasnain and Donald (16) could not be tracked in the present data due to limited temporal resolution.

Along with the reorientation of its principal directions, the magnitude of Γ polarizes spatially within the cell to become more compliant to shear in the downstream part as compared to the upstream part. This effect is probably related to a preferential relocation of focal adhesions and enhancement of cytoskeletal assemblies in the upstream region of the cells (4). A polarity of cell rheological properties has been observed previously. AFM measurements (11) revealed stiffening in the upstream part of the cells; it is to be noted that AFM studies measure stiffness in the normal direction rather than the planar direction in the current study.

The observed anisotropic nature of the microrheological properties of the cell produced by directional remodeling may provide the mechanism of directional mechanosensing and mechanotransduction necessary for the VECs to regulate their signaling and functions in response to changes in the magnitude and direction of the external forces imposed by blood flow on these cells.

Materials and Methods

Cell Culture, Flow Chamber and Microscopy. Bovine aortic endothelial cells (BAECs) were maintained in DMEM (DMEM) (Invitrogen) containing 25 mM Hepes and supplemented with 10% calf serum advantage (JR Scientific Inc.) in a humidified 5% CO_2/95% air incubator at 37 °C until confluency. The confluent BAECs were seeded on 50 × 35 mm coverslips coated with fibronectin (FN, Sigma) for 18–24 h. The cell-containing coverslip was assembled into the flow chamber, in which a rectangular flow channel (0.025 cm high, 1 cm wide, and 3 cm long) was created by sandwiching a silicon gasket between the coverslip (with the confluent BAECs) and a glass plate. Shear flow through the channel was generated by hydrostatic pressure difference between two reservoirs. The system was kept at 37 °C in a constant temperature hood, and the circulating medium was ventilated with humidified 5% CO_2/95% air. The ECs were subjected to a constant LSS of 16 dyn/cm^2 for 24 h and monitored under an Olympus IX70 microscope (Olympus America Inc. SEG). The control cell culture was kept for 24 h without being subjected to flow. Particle images were acquired at a rate of 5–9 frames/s for 5 min at 30-min intervals for 24 h using Simple PCI (Hamamatsu Corp.). The tracked particles have been identified as mitochondria by comparison with immunostained fluorescence images in which the mitochondria were labeled with the living cell dye MitoTracker Green FM (Invitrogen, see Fig. 1).

Directional Particle Tracking Microrheology. We used DPTM to determine viscoelastic properties of cytoplasm along different directions by measuring the two-dimensional (2D) correlation tensor of the random displacement of endogenous particles. This 2 × 2 tensor is

$$T_{i,j}(\tau) = \langle r_i(\tau) r_j(\tau) \rangle \qquad [2]$$

where $i, j = 1$ correspond to the first direction of the reference system, and $i, j = 2$ the second direction. In Eq. 2, $\vec{r}(\tau) = (r_1, r_2) = \vec{r}(t + \tau) - \vec{x}(\tau)$ is the displacement vector, where $\vec{x}$ is particle position, and τ is time separation between successive observations. The theoretical basis for DPTM stems from the application of a Langevin equation to the 2D random motion of a sphere in an orthotropic medium that opposes a frequency-dependent resistance, which is linearly proportional to the velocity of the sphere and can vary with the direction of motion. The eigenvalues of $T_{ij}(\tau)$, hereafter denoted r_+^2 and r_-^2, or principal mean square displacements (PMSD), provide the maximum and minimum values, respectively, of the creep[‖] compliance (Γ) along the two principal directions,

$$\Gamma_{+,-}(\tau) = \frac{\pi R}{K_B T} r_{+,-}^2(\tau), \qquad [3]$$

where R is particle radius, K_B is Boltzmann constant, and T is absolute temperature. The eigenvectors of $T_{ij}(\tau)$ provide the orientation of the principal directions of Γ (16).

[‖]"Creep" is a slow, progressive deformation of a material under constant stress. For example, in one dimension, consider the application of a stress $\sigma(t) = \sigma_0 H(t)$, where $H(t)$ is the Heaviside step function ($H(t) = 1$ for $t > 0$ and $H(t) = 0$ otherwise). This load leads to a strain $\varepsilon(t)$ in the material. The ratio $\Gamma(t) = \varepsilon(t)/\sigma_0$, is the creep compliance, which is independent of the stress level for linear materials. In elastic (solid-like) materials in which strain follows immediately to the application or release of stresses, the creep compliance is $\Gamma(t) = \Gamma_0 H(t)$ and the constant Γ_0 is the elastic compliance. In viscous (liquid-like) materials, the creep compliance grows with time as $\Gamma(t) = \eta t H(t)$, where η is the viscosity.

CELL BIOLOGY

The particles were tracked from time-lapse sequences of phase-contrast microscopy images using standard procedures (34). Digital processing of the images was performed with custom-written functions in MATLAB (The MathWorks). To determine whether the particle was undergoing active transport or passive diffusion, the MSD of each particle were fit to the curve:

$$\mathrm{MSD} = V^2\tau^2 + D\tau, \qquad [4]$$

where V is a persistent velocity and D is a diffusion coefficient. Particles undergoing active transport ($V > 0$) show an increased anisotropy of MSD distribution with increasing τ (see Fig. 2 in *Results*), and such particles were removed from the calculation of Γ.

ACKNOWLEDGMENTS. This work was supported by National Institutes of Health Grants 1R01 HL080518 and BRP HL064382. JCdÁ has been partially supported by the Spanish MEC (Fulbright Program).

1. Fung YC, Liu SQ (1993) Elementary mechanics of the endothelium of blood vessels. *J Biomech Eng* 115:1–12.
2. Levesque MJ, Nerem RM (1985) The elongation and orientation of cultured endothelial cells in response to shear stress. *J Biomech Eng* 107:341–347.
3. Galbraith CG, Skalak R, Chien S (1998) Shear stress induces spatial reorganization of the endothelial cell cytoskeleton. *Cell Motility and the Cytoskeleton* 40:317–330.
4. Davies PF, Robotewskyj A, Griem ML (1994) Quantitative studies of endothelial cell adhesion. Directional remodeling of focal adhesion sites in response to flow forces. *J Clin Invest* 93:2031–2038.
5. DePaola N, *et al.* (1999) Spatial and temporal regulation of gap junction connexin43 in vascular endothelial cells exposed to controlled disturbed flows in vitro. *Proc Natl Acad Sci USA* 96:3154–3159.
6. Wang N, Butler JP, Ingber DE (1993) Mechanotransduction across the cell surface and through the cytoskeleton. *Science* 260:1124–1127.
7. Chen CS, Tan J, Tien J (2004) Mechanotransduction at cell-matrix and cell–cell contacts. *Annu Rev Biomed Eng* 6:275–302.
8. Chien S (2007) Mechanotransduction and endothelial cell homeostasis: The wisdom of the cell. *Am J Physiol Heart Circ Physiol* 292:H1209–H1224.
9. Sato M, Ohshima N, Nerem RM (1996) Viscoelastic properties of cultured porcine aortic endothelial cells exposed to shear stress. *J Biomech* 29:461–467.
10. Helmke BP (2005) Molecular control of cytoskeletal mechanics by hemodynamic forces. *Physiology (Bethesda)* 20:43–53.
11. Sato M, Nagayama K, Kataoka N, Sasaki M, Hane K (2000) Local mechanical properties measured by atomic force microscopy for cultured bovine endothelial cells exposed to shear stress. *J Biomech* 33:127–135.
12. Dangaria JH, Butler PJ (2007) Macrorheology and adaptive microrheology of endothelial cells subjected to fluid shear stress. *Am J Physiol Cell Physiol* 293:C1568–C1575.
13. Lee JS, *et al.* (2006) Ballistic intracellular nanorheology reveals ROCK-hard cytoplasmic stiffening response to fluid flow. *J Cell Sci* 119:1760–1768.
14. Mason TG, Weitz DA (1995) Optical measurements of frequency-dependent linear viscoelastic moduli of complex fluids. *Phys Rev Lett* 74:1250–1253.
15. Tseng Y, Kole T, Wirtz D (2002) Micromechanical mapping of live cells by multiple-particle-tracking microrheology. *Biophys J* 83:3162–3176.
16. Hasnain IA, Donald AM (2006) Microrheological characterization of anisotropic materials *Physical Review E* 73:031901.
17. Lin A, Krockmalnic G, Penman S (1990) Imaging cytoskeleton–mitochondrial membrane attachments by embedment-free electron microscopy of saponin-extracted cells. *Proc Natl Acad Sci USA* 87:8565–8569.
18. Wang N, *et al.* (2001) Mechanical behavior in living cells consistent with the tensegrity model. *Proc Natl Acad Sci USA* 98:7765–7770.
19. Hu S, *et al.* (2003) Intracellular stress tomography reveals stress focusing and structural anisotropy in cytoskeleton of living cells. *Am J Physiol Cell Physiol* 285:C1082–C1090.
20. Knowles MK, Guenza MG, Capaldi RA, Marcus AH (2002) Cytoskeletal-assisted dynamics of the mitochondrial reticulum in living cells. *Proc Natl Acad Sci USA* 99:14772–14777.
21. Hoffman, BD, Massiera, G, Van Citters, KM, Crocker, JC (2006) The consensus mechanics of cultured mammalian cells. *Proc Natl Acad Sci USA* 103:10259–10264.
22. Han Y, *et al.* (2006) Brownian motion of an ellipsoid. *Science* 314:626–630.
23. Fabry B, *et al.* (2001) Scaling the microrheology of living cells. *Phys Rev Lett* 87:148102.
24. Hu S, *et al.* (2004) Mechanical anisotropy of adherent cells probed by a three-dimensional magnetic twisting device. *Am J Physiol Cell Physiol* 287:C1184–1191.
25. Karcher H, *et al.* (2003) A three-dimensional viscoelastic model for cell deformation with experimental verification. *Biophys J* 85:3336–3349.
26. Tseng Y, Lee JS, Kole TP, Jiang I, Wirtz D (2004) Micro-organization and visco-elasticity of the interphase nucleus revealed by particle nanotracking. *J Cell Sci* 117:2159–2167.
27. Kole TP, Tseng Y, Jiang I, Katz JL, Wirtz D (2005) Intracellular mechanics of migrating fibroblasts. *Mol Biol Cell* 16:328–338.
28. Stamenovic D, *et al.* (2007) Rheological behavior of living cells is timescale-dependent. *Biophys J* 93:39–41.
29. Mizuno D, Tardin C, Schmidt CF, Mackintosh FC (2007) Nonequilibrium mechanics of active cytoskeletal networks. *Science* 315:370–373.
30. MacKintosh FC, Levine AJ (2008) Nonequilibrium mechanics and dynamics of motor-activated gels. *Phys Rev Lett* 100:018104.
31. Wechezak AR, Viggers RF, Sauvage LR (1985) Fibronectin and F-actin redistribution in cultured endothelial cells exposed to shear stress. *Lab Invest* 53:639–647.
32. Girard PR, Nerem RM (1993) Endothelial cell signaling and cytoskeletal changes in response to shear stress. *Front Med Biol Eng* 5:31–36.
33. Osborn EA, Rabodzey A, Dewey CF, Jr., Hartwig JH (2006) Endothelial actin cytoskeleton remodeling during mechanostimulation with fluid shear stress *Am J Physiol Cell Physiol* 290:C444–C452.
34. Crocker JC, Grier DG (1996) Methods of digital video microscopy for colloidal studies. *J Colloid Interface Sci* 179:298–310.